



## Growth of Dome-Shaped Carbon Nanoislands on Ir(111): The Intermediate between Carbidic Clusters and Quasi-Free-Standing Graphene

Paolo Lacovig,<sup>1,4</sup> Monica Pozzo,<sup>2</sup> Dario Alfè,<sup>2</sup> Paolo Vilmercati,<sup>3,4</sup> Alessandro Baraldi,<sup>4,5,\*</sup> and Silvano Lizzit<sup>1</sup>

<sup>1</sup>*Sincrotrone Trieste, Strada Statale 14 Km 163.5, 34012 Trieste, Italy*

<sup>2</sup>*Department of Earth Sciences, Department of Physics and Astronomy, and London Centre for Nanotechnology, University College London, Gower Street, London WC1E 6BT, United Kingdom*

<sup>3</sup>*Department of Physics and Astronomy, University of Tennessee, Knoxville, Tennessee 37996, USA*

<sup>4</sup>*Physics Department, University of Trieste, Via Valerio 2, I-34127 Trieste, Italy*

<sup>5</sup>*Laboratorio TASC INFN-CNR, S.S. 14 Km 163.5, I-34012 Trieste, Italy*

(Received 14 May 2009; published 12 October 2009; corrected 15 October 2009)

By combining high-resolution photoelectron spectroscopy and *ab initio* calculations, we show that carbon nanoislands formed during the growth of a long-range ordered graphene layer on Ir(111) assume a peculiar domelike shape. The understanding of the unusual growth mechanism of these C clusters, which represent an intermediate phase between the strongly coupled carbidic carbon and a quasi-free-standing graphene layer, can provide information for a rational design of graphenelike systems at the nanoscale.

DOI: 10.1103/PhysRevLett.103.166101

PACS numbers: 68.65.-k, 61.46.Bc, 81.05.Uw

The rising interest of the scientific community in graphene is motivated by its special and unique physical properties which make it one of the most promising materials for applications in nanoelectronics [1,2], electrochemistry [3], and gas sensing [4]. Its growth by means of hydrocarbon dissociation on transition metal (TM) surfaces represents a challenging way to its synthesis. Peculiar mechanisms of graphene growth, strikingly different from those observed for two-dimensional metal islands on metals, have been found depending on the metal substrate. On Ru graphene sheets increase their size by adding rare clusters of about 5 C atoms rather than monomers [5], while on Ir the islands coalescence takes place via Smoluchowski ripening, with entire C islands moving on the surface at high temperature [6].

A crucial point of the graphene-TM systems is the strength of the interaction with the different metal substrates. Recent studies have shown that by going from 5d to 4d TM the interaction of graphene changes from a weak to strong chemical bond with the substrate [7]. In this context the (111) Ir surface deserves special attention for two reasons: (i) the unparalleled structural quality of the graphene layer grown on this surface, as observed with scanning tunneling microscopy (STM) [8,9], and (ii) the small interaction of graphene with this substrate as judged by photoemission measurements showing a single, narrow C 1s component [7] and the energy position of the Dirac point close to the Fermi level [10].

A fundamental issue, not yet addressed in the onset of graphene formation, relates to the processes that bring carbidic clusters to develop into a graphene island. It is evident that lattice mismatch and island size play a crucial role, but very little is known about the atomic-scale mechanisms of the transition from strong- to weak-interacting C layers, an important target for tailoring the properties of

graphene-based nanoscale devices in a controlled and reproducible way. In this Letter, we report on the relationship between the interaction of C clusters with the metal substrate and their morphology in the initial stage of graphene formation on Ir(111). Using *in situ* high-resolution photoelectron spectroscopy in combination with density functional theory (DFT) calculations, we found that the weak interaction of the perfectly ordered graphene layer with the substrate does not affect appreciably the Ir 4f<sub>7/2</sub> surface core level shift (SCLS) with respect to the clean surface. On the contrary, the presence of C clusters differently bound to the surface gives rise to distinguished components in both the C 1s and Ir 4f<sub>7/2</sub> core levels. Their behavior as a function of C concentration and substrate temperature highlights the mechanisms that bring dome-shaped C nanoislands to the formation of an almost free-standing graphene layer.

The photoemission experiments were performed at the SuperESCA beam line [11] of the ELETTRA synchrotron radiation source. The fast data acquisition time combined with the high sensitivity to the local environment of C 1s and Ir 4f<sub>7/2</sub> core levels allowed us to probe *in situ* the modification in the C-cluster/substrate interaction during graphene growth. C atoms were obtained by dosing C<sub>2</sub>H<sub>4</sub> at pressures ranging from 10<sup>-9</sup> to 10<sup>-6</sup> mbar and in the temperature range 300–1270 K. Core level spectra were measured also at room temperature after each deposition cycle and at different intermediate coverage. The spectra were fitted using Doniach-Šunjić functions convoluted with Gaussians [12]. The DFT calculations were performed with the VASP code [13], using the projector-augmented wave method [14,15], the Perdew-Burke-Ernzerhof exchange-correlation functional [16], and an efficient extrapolation for the charge density [17]. Single particle orbitals were expanded in plane waves, with a

cutoff of 400 eV. SCLSs were calculated in the final state approximation [18]. For the clean surface, we used up to 9 atomic layers, even though with 5 layers the SCLSs converged to within  $\sim 10$  meV [19].

As a first step we compared the Ir  $4f_{7/2}$  spectrum of clean Ir(111) with that of the graphene/Ir interface. Graphene was prepared by repeated cycles of  $C_2H_4$  dosing at 300 K and subsequent annealing to 1470 K, which ensures the formation of a long-range ordered layer [10]. Figure 1(a) shows the Ir  $4f_{7/2}$  core level spectrum of the clean Ir(111). Because of the reduced coordination of first-layer Ir atoms with respect to the bulk, the surface component moves to a lower binding energy. The measured SCLS is  $-545$  meV, in good agreement with Ref. [20] and with our DFT result of  $-550$  meV.

The Ir  $4f_{7/2}$  spectrum corresponding to the best graphene layer, reported in Fig. 1(b), is very similar to that of the clean surface with a SCLS of  $-535$  meV. This is surprising since it is well known that a small amount of impurities induces substantial variations in spectral position and line shape, while here the presence of a large amount of carbon leaves the Ir spectrum practically unchanged. This result is a direct indication that the interaction between graphene and Ir(111) is very small: Any

modification in the electronic properties due to charge transfer, surface hybridization, or core-hole screening are expected to produce significant and measurable SCLSs.

This interpretation is further corroborated by the DFT results of the Ir  $4f_{7/2}$  SCLS. Figure 1(b) shows the calculated geometry of a graphene layer on Ir(111), with the typical moiré pattern with a corrugation of  $0.3$  Å [8,9]. The structure is obtained by overlaying a graphene layer at  $3$  Å from the Ir surface and relaxing the top two Ir layers together with the graphene layer [21]. Because of the corrugation of graphene, first-layer Ir atoms are in principle not all equivalent. To compare experimental and theoretical SCLSs we have therefore computed this quantity for two different Ir atoms: one right below a C atom (hcp region) and one below the center of a hexagon of C atoms (top region). They present SCLSs of  $-551$  and  $-549$  meV, respectively, in good agreement with the experimental findings, confirming that graphene does not affect the Ir surface appreciably.

To shed light on the evolution of the clusters-substrate interaction prior to the growth of a perfect graphene layer, we monitored the evolution of the C  $1s$  and Ir  $4f_{7/2}$  spectra (i) upon annealing to different temperatures the surface saturated with  $C_2H_4$  at 300 K and (ii) during  $C_2H_4$  exposure at 820, 970, and 1270 K. These two procedures result in different morphologies of the C clusters, as seen with STM [6]: While in the second case the clusters grow exclusively at step edges because of rapid C diffusion and occupation of preferred configurations, in the first case flat C island formation takes place also on the terraces, and an overall coverage of 0.29 ML is obtained.

The C  $1s$  and Ir  $4f_{7/2}$  spectra of the first procedure are shown in Fig. 2. The appearance of three components at  $284.12(C_A)$ ,  $283.94(C_B)$ , and  $283.61(C_C)$  eV in the C  $1s$  spectra reflects the presence of inequivalent C species that behave differently upon increasing temperature. While  $C_A$  and  $C_C$  remain at the same binding energy (BE) and their intensity is just reduced,  $C_B$  increases in intensity and moves progressively towards higher BE, to end up at the same BE of the graphene layer of  $284.10$  eV. The analysis of the peak intensities reveals that the decrease of  $C_C$  corresponds to the increase of  $(C_A + C_B)$ . We will show below that this is due to the change of the morphology of the C clusters. The Ir  $4f_{7/2}$  spectra reported in Fig. 2 for the same experiment present the bulk component together with the peak of the clean or graphene covered surface and a third, broad feature between the two due to a new first-layer population of Ir atoms interacting differently with the C clusters. Upon increasing the temperature this peak shows a SCLS that changes from  $-225$  meV at 820 K to  $-390$  meV at 1270 K and progressively diminishes in intensity.

The most significant results of the second dosing procedure arise from time-lapsed C  $1s$  spectra measured at 820 K [22], which can be fitted using the same three

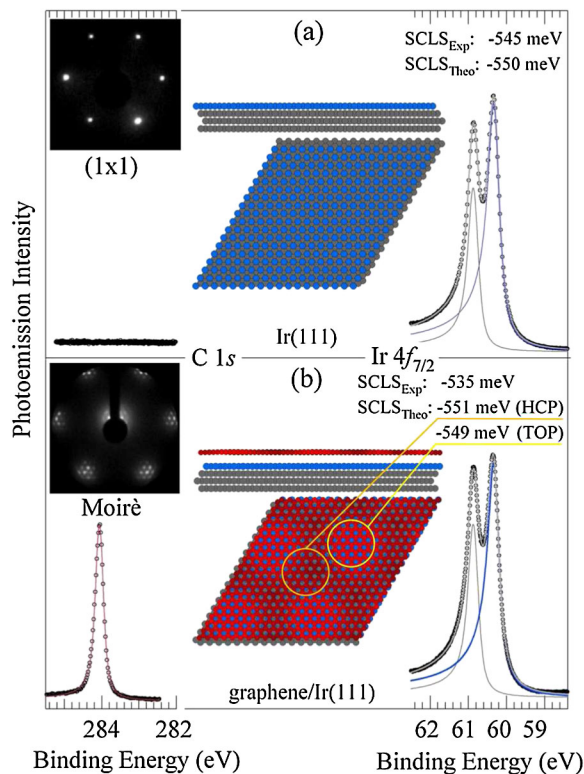


FIG. 1 (color online). C  $1s$  (left) ( $h\nu = 400$  eV) and Ir  $4f_{7/2}$  (right) ( $h\nu = 130$  eV) core level spectra and top and side views of the calculated structural models of (a) clean Ir(111) and (b) the graphene layer on Ir(111). The moiré corrugation of the graphene layer is displayed in red with different brightnesses. Low energy electron diffraction patterns are also shown.

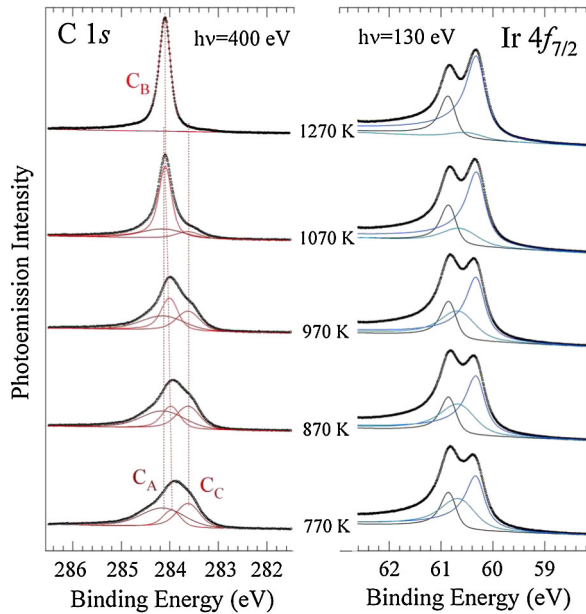


FIG. 2 (color online). C  $1s$  (left) and Ir  $4f_{7/2}$  (right) spectra after annealing at different temperatures of the Ir(111) surface saturated with  $C_2H_4$  at 300 K. The spectra were measured at 300 K. The different components represent inequivalent C and Ir atoms, as explained in the text.

components of the annealing experiment, plus a fourth component,  $C_S$  at 283.35 eV BE, which is compatible with the existence of C atoms at the Ir steps, in good agreement with STM results [6]. Most importantly, the uptake experiments show that the graphene layer is formed even at low C coverage when  $C_2H_4$  is dosed above 970 K. As for the C  $1s$  data at 820 K, the Ir  $4f_{7/2}$  results indicate that in the whole coverage range until saturation the interaction between Ir and C islands remains rather large if compared with the ordered graphene layer case.

To explain the origin of the differences in cluster-substrate interaction arising at different temperature and C coverage, we performed DFT calculations of the C-cluster morphology evolution with cluster size. We mapped the structure of the clusters formed with different number  $n$  of honeycomb rings (HRs), the graphene building blocks, with an overall number of 6 ( $n = 1$ ), 13 ( $n = 3$ ), 24 ( $n = 7$ ), and 54 ( $n = 19$ ) C atoms, respectively. The geometry of the clusters was determined by full relaxation after short simulated annealing.

The structural models obtained are shown in Fig. 3. The geometry of a single HR [Fig. 3(a)] is quite simple: The C atoms, placed in bridge sites, sit in a planar configuration with a C-Ir distance of 1.62 Å and the symmetry axes oriented along the  $[10\bar{1}]$  direction. The increase of  $n$  has drastic effects on cluster morphology. The cluster with  $n = 3$  [Fig. 3(b)] abandons the flat configuration and bends upwards assuming a dome-like shape: The central C atom is now at a distance of 2.53 Å from the Ir surface, and only

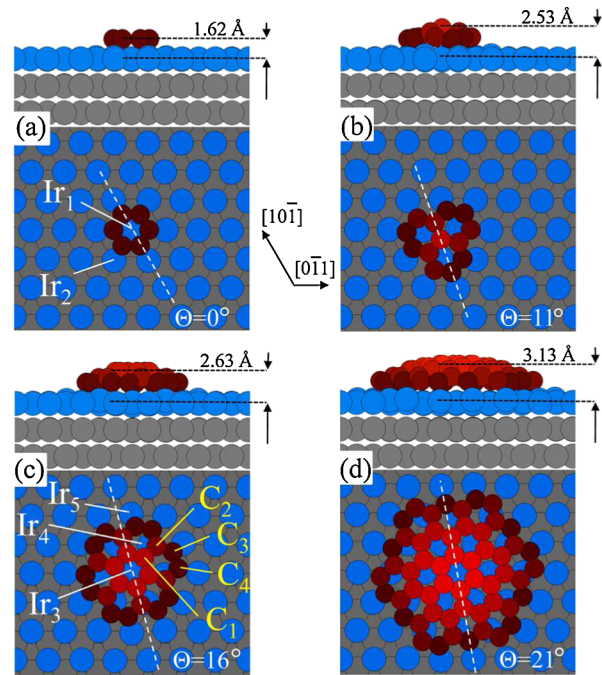


FIG. 3 (color online). Calculated structural models of the C clusters formed by  $n$  honeycomb rings with (a)  $n = 1$ , (b)  $n = 3$ , (c)  $n = 7$ , and (d)  $n = 19$ .  $Ir_i$  ( $i = 1, \dots, 6$ ) and  $C_j$  ( $j = 1, \dots, 4$ ) represent different Ir and C local configurations, respectively, as explained in the text. The distance of the central C atoms from the Ir substrate as well as the orientation of the cluster with respect to the  $[10\bar{1}]$  direction of Ir(111) are also shown.

the C atoms at the periphery remain close to the Ir substrate. This process is paralleled by a rotation of the symmetry axes by  $11^\circ$ . For larger cluster sizes the unsticking process goes on further: The top C atoms for  $n = 7$  and  $n = 19$  move apart by 2.63 and 3.13 Å, respectively, while the cluster undergoes further rotation, not too far from the value of  $30^\circ$  of a graphene layer with a C-C distance of 1.42 Å.

We then computed the Ir  $4f_{7/2}$  and C  $1s$  CLS for some of the clusters of Fig. 3 and compared them with the experimental results. For  $n = 1$  and  $n = 7$  we calculated the CLS of representative Ir and C local configurations, indicated with labels  $Ir_i$  ( $i = 1, \dots, 5$ ) and  $C_j$  ( $j = 1, \dots, 4$ ) in Fig. 3. For  $n = 1$ ,  $Ir_1$  and  $Ir_2$  display a SCLS of  $-325$  and  $+498$  meV, respectively. The absence in the experiments of Ir  $4f_{7/2}$  components with BE larger than the bulk one suggests that this local configuration is not present. However, moving to  $n = 7$ , the calculated SCLSs are  $-551$ ,  $-132$ , and  $-270$  meV for  $Ir_3$ ,  $Ir_4$ , and  $Ir_5$ , respectively. This finding clearly indicates that even for a very small C island the interaction of the Ir atoms placed just below the center of the dome ( $Ir_3$ ) is very small, the SCLS being the same as for the clean Ir(111) and graphene/Ir(111) surfaces. Only the Ir atoms directly bonded with the C atoms at the cluster edge strongly

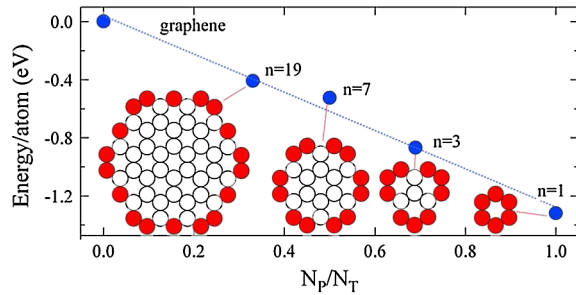


FIG. 4 (color online). Evolution of the binding energy/atom as a function of the ratio of C atoms at the periphery  $N_p$  and the total number  $N_T$  in each C cluster.

interact with C and present SCLSs that fall in the BE region of the broad extra component needed to fit the Ir  $4f_{7/2}$  spectra. The C  $1s$  CLSs for  $n = 7$  of  $C_2$ ,  $C_3$ , and  $C_4$  atoms calculated with respect to the  $C_1$  configuration are +268, -348, and -439 meV, respectively. The comparison with the experimental results allowed us to distinguish three different types of C atoms: The atoms at the periphery of the cluster bonded to 2 C atoms show a negative CLS as for  $C_C$ , and C atoms bonded with 3 C atoms and directly bonded to the periphery atoms show a positive CLS as for  $C_A$ . Finally, the atoms at the center of the cluster originate the  $C_B$  component.

The close correspondence of experimental and theoretical CLS results suggest that, while growing, the C clusters remain strongly bonded to the substrate only at the periphery ( $C_C$  atoms) as a result of the C  $2p$  hybridization with the first-layer Ir  $d$  band. Because of island diffusion and coalescence via Smoluchowski ripening [6], the cluster size increases with temperature and the ratio  $N_p/N_T$  decreases ( $N_p$  is the number of atoms at the periphery, and  $N_T$  is the total number of atoms in the cluster). This is in very good agreement with the behavior reported in Fig. 2: Small compact islands with a large number of atoms at the edge ( $C_C$ ) and near edge ( $C_A$ ) nucleate to form large islands at 1270 K. At this temperature the relative population of  $C_A$  and  $C_C$  species is on the order of 0.1%, i.e., below our sensitivity limit. The narrowing of  $C_B$  with increasing temperature directly correlates with the calculated distribution of C-C distances that gets narrower and moves towards the 1.421 Å value found for graphene, with increasing cluster size.

To further support our interpretation about the role of the atoms at the cluster edge, we report in Fig. 4 the evolution of the calculated binding energy/atom in the cluster as a function of  $N_p/N_T$  for different cluster sizes. The graph displays a remarkable linear behavior and indicates that the islands are bonded to the substrate mainly with the C atoms at the edges. This gives further support to the importance of the correlation between the bonding interaction of the cluster and the number of atoms at the periphery.

In conclusion, we have shown that the transition from carbidic C to a low interacting graphene layer proceeds via formation of dome-shaped C nanoislands whose interaction with the Ir substrate takes place only at the cluster edge. The new mechanism of cluster growth, which results in nanosized noninteracting C regions, offers the groundwork for a rational nanoscale design of graphenelike systems, such as quantum dots and nanoribbons.

The work of M. P. and D. A. was conducted as part of the EURYI scheme program as provided by EPSRC (see [23]). Calculations were performed on the HECToR national service.

\*alessandro.baraldi@elettra.trieste.it

- [1] A. H. Castro Neto *et al.*, Rev. Mod. Phys. **81**, 109 (2009).
- [2] T. Ohta *et al.*, Science **313**, 951 (2006).
- [3] D. C. Elias *et al.*, Science **323**, 610 (2009).
- [4] N. G. Ahang *et al.*, Adv. Funct. Mater. **18**, 3506 (2008).
- [5] E. Loginova, N. C. Bartelt, P. J. Feibelman, and K. F. McCarty, New J. Phys. **10**, 093026 (2008).
- [6] J. Coraux *et al.*, New J. Phys. **11**, 023006 (2009).
- [7] A. B. Preobrajenski, M. L. Ng, A. S. Vinogradov, and N. Mårtensson, Phys. Rev. B **78**, 073401 (2008).
- [8] A. T. N'Diaye, S. Bleikamp, P. J. Feibelman, and T. Michely, Phys. Rev. Lett. **97**, 215501 (2006).
- [9] A. T. N'Diaye *et al.*, New J. Phys. **10**, 043033 (2008).
- [10] I. Pletikoscic *et al.*, Phys. Rev. Lett. **102**, 056808 (2009).
- [11] A. Baraldi *et al.*, Surf. Sci. Rep. **49**, 169 (2003).
- [12] S. Doniach and M. Šunjić, J. Phys. C **3**, 285 (1970).
- [13] G. Kresse and J. Furthmüller, Phys. Rev. B **54**, 11 169 (1996).
- [14] P. E. Blöchl, Phys. Rev. B **50**, 17 953 (1994).
- [15] G. Kresse and J. Joubert, Phys. Rev. B **59**, 1758 (1999).
- [16] J. P. Perdew, K. Burke, and M. Ernzerhof, Phys. Rev. Lett. **77**, 3865 (1996).
- [17] D. Alfè, Comput. Phys. Commun. **118**, 31 (1999).
- [18] S. Lizzit *et al.*, Phys. Rev. B **63**, 205419 (2001).
- [19] The adsorption of graphene has been modeled by overlaying a  $10 \times 10$  graphene sheet over a  $9 \times 9$  Ir(111) supercell and a slab of 4 Ir layers, using the  $\Gamma$  point only. Using a  $2 \times 2 \times 1$   $k$ -point grid or 5 layers only changes differences in the SCLS by  $\sim 1$  meV and the equilibrium distance between the graphene layer and the Ir surface by 0.002 Å.
- [20] M. Bianchi *et al.*, New J. Phys. **11**, 063002 (2009).
- [21] The relaxation was stopped when the total energy converged to less than  $10^{-5}$  eV and the forces on all of the atoms to less than 0.005 eV/Å. Such a tight convergence requirement is needed because during the relaxation the graphene layer tends to move away from the surface, and eventually it ends up at a distance of  $\sim 4$  Å.
- [22] See EPAPS Document No. E-PRLTAO-103-060940 for the uptakes experiments. For more information on EPAPS, see <http://www.aip.org/pubservs/epaps.html>.
- [23] <http://www.esf.org/euryi>.